Eur. Phys. J. A **16**, 495–507 (2003)
DOI 10.1140/epja/i2002-10122-9

THE EUROPEAN PHYSICAL JOURNAL A

Charge distribution studies in the fast-neutron–induced fission of ^{232}Th, ^{238}U, ^{240}Pu and ^{244}Cm

H. Naik, R.J. Singh, and R.H. Iyer[a]

Radiochemistry Division, Bhabha Atomic Research Centre, Trombay, Mumbai-400 085, India

Received: 26 July 2002 / Revised version: 13 November 2002 /
Published online: 3 April 2003 –
Communicated by D. Schwalm

Abstract. Charge distribution studies for heavy-mass fission products were carried out in the fast-neutron–induced fission of ^{232}Th, ^{238}U, ^{240}Pu and ^{244}Cm using radiochemical and gamma-ray spectrometric techniques. The width parameter(σ_Z/σ_A), the most probable charge/mass (Z_P/A_P), the charge polarization (ΔZ) and the slope of charge polarization [$\delta(\Delta Z)/\delta A'$] as a function of the fragment mass (A') were deduced. The average charge dispersion parameter ($\langle\sigma_Z\rangle$) and proton odd-even effect (δ_p) were also obtained for these fissioning systems. The $\langle\sigma_Z\rangle$ and δ_p values in the fissioning systems ^{241}Pu* and ^{245}Cm* were determined for the first time. The $\delta(\Delta Z)/\delta A'$ value is also determined for the first time in the fissioning systems ^{239}U*, ^{241}Pu* and ^{245}Cm*. These data along with the literature data for even-Z fissioning systems such as ^{230}Th*, ^{232}Th*, ^{233}U*, ^{234}U*, ^{236}U*, ^{238}U*, ^{239}Pu*, ^{240}Pu$*$, ^{242}Pu*, ^{246}Cm*, ^{250}Cf* and ^{252}Cf(SF) are discussed in terms of nuclear structure effect and dynamics of descent from the saddle to the scission point. The role of the excitation energy in low-energy fission is also discussed.

PACS. 25.85.Ec Neutron-induced fission

1 Introduction

Studies on the charge distribution in the low-energy fission of actinides provide important information on the fission process such as the effect of nuclear structure and the dynamics of descent from saddle to scission. It also provides information about the quasi-particle excitation, *i.e.* whether it takes place at second saddle or during the descent from second saddle to scission or during neck snapping. Experimental investigations on charge distribution have been carried out using physical methods based on i) measurements of beta chain lengths, *i.e.* number of successive beta emissions from the mass-separated products [1,2], ii) multiparameter coincidence measurements of either K X-rays intensities (yields) of fission products [3] or the intensity of ground-state rotational band transitions of even-even fission products [4] in conjunction with the kinetic energy of the complementary fragments and iii) online mass spectrometric measurements [5–7]. The above physical methods were used for the charge distribution studies of both light- and heavy-mass fission products in a limited number of fissioning systems. However, the other physical methods based on iv) ΔE-E_R telescopes [8,9], v) E_1-E_2 detectors [10], vi) the fission product recoil mass separator [11–17] and the COSIFANTUTTE spectrometer [18–20] were used exhaustively for the charge distribution studies of light-mass fission products in the thermal-neutron–induced fission of ^{229}Th to ^{249}Cf and ^{252}Cf(SF). On the other hand, the charge distribution studies using radiochemical and gamma spectrometric techniques were carried out for both light- and heavy-mass fission products in many fissioning systems [21–48] but are exhaustive only for the fissioning systems ^{230}Th*, ^{234}U*, ^{236}U*, ^{240}Pu*, ^{242}Pu*, ^{246}Cm* and ^{252}Cf(SF) [21,39]. A detailed work on charge distribution studies carried out so far in low-energy fission has been summarized by Vandenbosch and Huizenga [49] as well as by Gonnenwein [50].

In the present work, charge distribution studies have been carried out in the fast-neutron–induced fission of ^{232}Th, ^{238}U, ^{240}Pu and ^{244}Cm using radiochemical and gamma spectrometric techniques. These data along with the literature data for other even-Z fissioning systems are discussed in terms of the effect of shell closure proximity, the odd-even effect and the dynamics of descent from saddle to the point of neck formation and from the latter to the point of scission. The role of excitation energy on charge distribution in low-energy fission is also discussed.

2 Experimental

A known amount of 25 μm thick ^{232}Th metal foil ($\sim$ 50 mg), electrodeposited targets of 99.9997 atom

[a] *Present address*: Emeritus Scientist (CSIR) Bhabha Atomic Research Centre, Nuclear Recycle Group, WIP Building, Trombay, Mumbai-400085, India; e-mail: rhiyer@magnum.barc.ernet.in

% ^{238}U ($\sim$ 500 μg), 99.48 atom % ^{240}Pu (96 μg) and 99.43 atom % ^{244}Cm (96 μg) were covered with either a 75 μm thick Lexan or a 25 μm thick aluminum foil which acted as a catcher to collect the recoiling fission products during neutron irradiation of the target. It was then wrapped with 1 mm thick cadmium foil, doubly sealed in alkathene bags and irradiated for 5 to 60 min in the highly enriched uranium-fueled light-water–moderated swimming pool reactor APSARA at a flux of 1.2×10^{12} n cm^{-2} s^{-1}. The cadmium wrapper served two purposes. In the case of ^{232}Th and ^{238}U it reduces the formation of ^{233}Th and ^{239}U and their daughter products ^{233}Pa and ^{239}Np from ^{232}Th(n,γ) and ^{238}U(n,γ) reactions, respectively, whose gamma-rays otherwise interfere with the gamma-ray spectrum of the fission products. In the case of ^{240}Pu and ^{244}Cm it also prevents the fissions due to thermal neutrons, since these actinide targets have 0.39% of ^{239}Pu and 0.0065% of ^{245}Cm, respectively, as thermal fission contaminants. After irradiation the aluminum catchers were dissolved in a dilute sodium hydroxide solution and iodine was separated using a standard radiochemical procedure [51]. On the other hand, the Lexan catcher foils were washed with very dilute nitric acid followed by distilled water for removing possible contamination of activation products from ^{232}Th and ^{238}U and alpha contamination of ^{240}Pu and ^{244}Cm. They were then mounted on a perspex plate. Lexan catcher foils on perspex plates as well as the aliquots of iodine samples in counting vials were counted in a fixed geometry on an energy and efficiency-calibrated 120 c.c. HPGe detector coupled to a PC-based 4096 channel analyzer. The resolution of the detector system was 1.8 keV at 1332 keV of ^{60}Co. In the above type of irradiation assemblies there is a possibility of escape of inert-gas fission products such as krypton and xenon. To prevent this escape as well as for a better assessment of short-lived fission products, $\sim$ 200 μl of ^{238}U (30.01 mg/ml), ^{240}Pu (0.507 mg/ml) and ^{244}Cm (0.55 mg/ml) in the form of nitrate solutions sealed in a polypropylene tube were covered with 1 mm thick cadmium foil and again sealed in two alkathene bags. The ^{238}U target was irradiated for 5 min in the same position of the reactor APSARA as described earlier. In the case of ^{240}Pu and ^{244}Cm, the targets were irradiated for 1 to 5 min using the pneumatic carrier facility of the heavy-water–moderated natural uranium-fueled CIRUS reactor at a flux of 2×10^{12} cm^{-2}s^{-1}. The neutron spectrum for the irradiation position of the rector APSARA and CIRUS were shown in our earlier work [30], from which the mean neutrons energies of the neutron beam was found to be 1.9 MeV. The irradiated targets were mounted as such on a perspex plate (without opening the tube) and then analyzed by gamma-ray spectrometry at a fixed geometry in an energy and efficiency calibrated 80 c.c. HPGe detector coupled to a PC-based 4096 channel analyzer. The resolution of the detector system was 2.0 keV at 1332 keV of ^{60}Co. The dead time of the detector system during counting was always kept less than 10% to avoid the pile-up effect. The gamma-ray counting of the samples was done in live time mode and was followed as a function of time for at least three half-lives. The gamma lines along with their nuclear spectroscopic data for different nuclides used in the present work were taken from refs. [52,53].

3 Calculations and results

The photopeak areas of different gamma-rays of the fission products were calculated from their total peak areas by subtracting the linear Compton background. From the photopeak areas the cumulative and independent yields of fission products relative to some internal fission product monitor were determined using decay-growth equations [21,41–44]. In the unseparated samples ^{104}Tc and ^{92}Sr were used as fission rate monitor for short and long-lived fission products, respectively. The absolute yields of these fission rate monitors were taken from refs. [27,30] where they were determined using track-etch cum gamma-ray spectrometric technique. In the radiochemically separated iodine samples ^{135}I was used as the fission rate monitor. The independent yields of iodine isotopes were determined from the knowledge of separation time activities and employing decay-growth equations [21,41–44] after correcting for the precursor contributions. The cumulative yields of fission products in the fast-neutron–induced fission of ^{232}Th, ^{238}U, ^{240}Pu and ^{244}Cm were converted to their fractional yields using the mass chain yields from refs. [54,55]. The fractional cumulative yields (FCY) of a few fission products were determined from the activities of the daughter products using the parent daughter genetic equation [21,41–44]. These FCY data and independent-yield values from the present work along with the available literature data [24–33] for different nuclides in the above fissioning systems are given in tables 1 and 2, respectively. The uncertainties shown on FCY values are the propagated errors due to errors on cumulative yields and mass chain yields, whereas the uncertainties quoted in the independent yields are the standard deviations of replicate measurements. Independent yields of some of the fission products given in brackets in table 2 are derived from their fractional cumulative yields or from the yields of parent and daughter fission products. These data from tables 1 and 2 are used to obtain the charge distribution parameters as follows.

3.1 Evaluation of charge distribution parameters

3.1.1 Isobaric yield distribution

In an isobaric mass chain, the yield distribution follows a Gaussian distribution [39]. Accordingly in a given isobaric mass chain the fractional cumulative yield (FCY) for a particular fission product of charge Z is given by

$$FCY = \frac{EOF^{a(Z)}}{\sqrt{2\pi\sigma_Z^2}} \int_{-\infty}^{Z+0.5} \exp[-(Z - Z_{\rm P})^2/2\sigma_Z^2]\mathrm{d}Z\,, \quad (1)$$

where $Z_{\rm P}$ is the most probable charge, σ_Z is the charge dispersion parameter of the isobaric yield distribution.

Table 1. Fractional cumulative yields of various fission products in ^{233}Th*, ^{239}U*, ^{241}Pu* and ^{245}Cm*.

Nuclide	^{233}Th*	Ref.	^{239}U*	Ref.	^{241}Pu*	Ref.	^{245}Cm*	Ref.
^{128}Sn	$0.967 \pm 0.015^{(a)}$	A	0.970 ± 0.014	A	0.638 ± 0.063	A	0.652 ± 0.086	A
			$0.982 \pm 0.018^{(a)}$	A	$0.676 \pm 0.063^{(a)}$	A		
^{129}Sb					0.990 ± 0.011	A	0.925 ± 0.041	A
^{130}Sn	0.837 ± 0.037	A	0.656 ± 0.051	A	0.269 ± 0.069	A	0.193 ± 0.055	A
^{130}Sb			0.988 ± 0.023	A	0.938 ± 0.195	A	0.845 ± 0.083	A
^{131}Sn	0.740 ± 0.220	[25]						
^{131}Sb	0.984 ± 0.005	A	0.930 ± 0.053	[33]	0.667 ± 0.028	A	0.598 ± 0.097	A
			0.963 ± 0.017	A	$0.674 \pm 0.032^{(a)}$	A		
^{131}Te			0.99969	[33]	0.991 ± 0.040	A	0.966 ± 0.034	A
^{132}Sn	0.560 ± 0.139	[26]						
^{132}Sb	0.890 ± 0.050	A	0.835 ± 0.075	A	0.494 ± 0.079	A	0.343 ± 0.048	A
^{132}Te			$0.9965 \pm 0.0001^{(a)}$	[33]	$0.980 \pm 0.004^{(a)}$	A	0.881 ± 0.057	A
^{133}Sb	0.640 ± 0.066	A	0.590 ± 0.043	[33]	0.318 ± 0.046	A	0.207 ± 0.043	A
			0.606 ± 0.012	A				
^{133}Te	0.95	[24]	0.971 ± 0.006	A	0.862 ± 0.035	A	0.709 ± 0.090	A
	0.995 ± 0.037	A						
^{134}Te	$0.970 \pm 0.030^{(a)}$	[26]	$0.899 \pm 0.040^{(a)}$	A	0.653 ± 0.028	A	0.438 ± 0.059	A
	0.984 ± 0.004	[24]	0.920 ± 0.013	[33]	$0.660 \pm 0.064^{(a)}$	A		
^{134}I					0.980 ± 0.025	A	0.939 ± 0.047	A
^{135}Te	$0.855 \pm 0.030^{(a)}$	[26]						
	0.838 ± 0.030	[26]						
^{135}I	$0.9980 \pm 0.0020^{(a)}$	A	$0.9865 \pm 0.0007^{(a)}$	A	$0.906 \pm 0.053^{(a)}$	A	0.746 ± 0.087	A
	0.9965 ± 0.0035	A			0.882 ± 0.052	A		
^{136}I	0.877 ± 0.055	A	0.936 ± 0.037	A	0.452 ± 0.053	A	0.429 ± 0.055	A
^{136}Xe	0.9999702	[25]	0.99986 ± 0.00001	[31]	$0.984 \pm 0.005^{(a)}$	A	$0.977 \pm 0.004^{(a)}$	A
	± 0.0000038							
^{137}Xe					0.915 ± 0.053	A	0.796 ± 0.036	A
^{138}Xe	0.977 ± 0.058	A	0.990 ± 0.008	[32]	0.830 ± 0.010	A	0.668 ± 0.035	A
	$0.990 \pm 0.022^{(a)}$	A	$0.892 \pm 0.072^{(a)}$	A				
^{138}Cs							0.983 ± 0.014	A
^{139}Xe	0.950 ± 0.010	[24]	0.948 ± 0.005	[31]				
	0.980 ± 0.037	[26]						
^{139}Cs			0.9998 ± 0.0061	[32]	0.977 ± 0.023	A	0.894 ± 0.013	A
^{140}Xe	0.817 ± 0.064	[25]	0.860 ± 0.020	[31]				
	0.854 ± 0.039	[24]						
	0.890 ± 0.020	[26]						
^{140}Cs	0.963 ± 0.017	A	0.9973 ± 0.0103	[32]	0.802 ± 0.092	A	0.717 ± 0.103	A
^{140}Ba					$0.9964 \pm 0.0015^{(a)}$	A	$0.988 \pm 0.012^{(a)}$	A
^{141}Xe	0.550 ± 0.050	[24]	0.580 ± 0.050	[31]				
^{141}Cs			0.910 ± 0.070	[32]				
^{141}Ba	0.9990 ± 0.0194	A			0.970 ± 0.041	A	0.931 ± 0.103	A
^{142}Xe	0.350 ± 0.010	[24]						
^{142}Cs			0.705 ± 0.030	[32]				
^{142}Ba	0.9712 ± 0.0470	A	0.986 ± 0.044	A	$0.952 \pm 0.070^{(a)}$	A	0.812 ± 0.083	A
					0.899 ± 0.053	A		
^{143}Xe	$> 0.110 \pm 0.040$	[24]	0.088 ± 0.003	[31]				
^{143}Cs			0.518 ± 0.100	[32]				
^{144}Xe			0.028 ± 0.005	[31]				
^{144}La	0.9990 ± 0.0281	A	0.9953 ± 0.064	A	0.960 ± 0.009	A	0.920 ± 0.044	A
^{146}Ce	$0.9954 \pm 0.0029^{(a)}$	A	$0.9980 \pm 0.0047^{(a)}$	A	$0.970 \pm 0.023^{(a)}$	A	$0.942 \pm 0.004^{(a)}$	A
^{148}Ce	0.909 ± 0.138	A	0.940 ± 0.161	A	0.710 ± 0.055	A	0.630 ± 0.169	A

A: present work.

(^{a}) Atoms of parent/(Atoms of parent + Atoms of daughter).

Table 2. Independent yields of various fission products in ^{233}Th*, ^{239}U*, ^{241}Pu* and ^{245}Cm*.

Nuclide	^{233}Th*	Ref.	^{239}U*	Ref.	^{241}Pu*	Ref.	^{245}Cm*	Ref.
^{128}Sn	0.141 ± 0.022	[25]	0.241 ± 0.020	A	0.419 ± 0.035	A	0.447 ± 0.087	A
^{129}Sn					0.547 ± 0.068	A	0.389 ± 0.067	A
^{130}Sn	0.554 ± 0.083	A	0.922 ± 0.070	A	0.496 ± 0.066	A	0.326 ± 0.064	A
^{131}Sn	1.149 ± 0.326	[26]	1.356 ± 0.321	A	(0.268)	A	(0.167)	A
^{132}Sn	1.520 ± 0.230	[25]	(1.104)	A	(0.120)	A	(0.080)	A
	1.535 ± 0.246	[26]						
	1.596 ± 0.403	[26]						
^{128}Sb	0.0056 ± 0.0014	[25]	0.021 ± 0.005	A	0.245 ± 0.014	A	0.422 ± 0.023	A
^{129}Sb					0.718 ± 0.059	A	0.837 ± 0.173	A
^{130}Sb	0.163 ± 0.072	A	0.866 ± 0.043	A	1.501 ± 0.251	A	1.241 ± 0.142	A
^{131}Sb	0.358 ± 0.327	[26]	1.826 ± 0.175	[33]	1.743 ± 0.058	A	1.262 ± 0.041	A
	0.372 ± 0.333	[26]	2.011 ± 0.150	A				
	0.385 ± 0.011	[24]						
^{132}Sb	0.957 ± 0.383	[26]	3.031 ± 0.345	A	2.260 ± 0.019	A	1.469 ± 0.212	A
	1.001 ± 0.278	[26]						
	0.925 ± 0.281	[26]						
^{133}Sb	2.253 ± 0.238	A	2.725 ± 0.290	[33]	1.651 ± 0.250	A	1.205 ± 0.277	A
			2.757 ± 0.327	A				
^{131}Te	0.028 ± 0.006	[25]	< 0.120	[33]	1.300 ± 0.119	A	1.447 ± 0.199	A
			0.145 ± 0.007	A				
^{132}Te	0.385 ± 0.178	A	0.754 ± 0.160	[33]	2.340 ± 0.020	A	2.477 ± 0.194	A
^{133}Te	1.543 ± 0.147	A	2.910 ± 0.180	A	3.024 ± 0.132	A	2.968 ± 0.374	A
^{134}Te	3.868 ± 0.389	[26]	4.769 ± 0.220	[33]	4.675 ± 0.157	A	2.853 ± 0.313	A
	3.686 ± 0.411	[26]	6.113 ± 0.115	A				
^{135}Te	4.145 ± 0.250	[26]						
	4.178 ± 0.233	[26]						
^{131}I			< 0.001	[33]			0.080 ± 0.020	A
^{132}I			0.018 ± 0.005	A	0.195 ± 0.020	A	0.547 ± 0.027	A
^{133}I	< 0.198	[24]	0.199 ± 0.040	[33]	1.744 ± 0.014	A	0.986 ± 0.258	A
^{134}I	0.161 ± 0.023	[26]	0.770 ± 0.070	[33]	3.529 ± 0.162	A	1.890 ± 0.137	A
	0.086 ± 0.021	[24]	0.989 ± 0.064	A	1.964 ± 0.202	A		
^{135}I	0.760 ± 0.150	[25]	1.900 ± 0.210	A	3.518 ± 0.335	A	3.723 ± 0.550	A
	0.891 ± 0.166	[26]			3.588 ± 0.335	A		
	0.825 ± 0.166	[24]						
^{136}I	1.880 ± 0.346	[24]	2.992 ± 0.503	A	3.002 ± 0.008	A	3.869 ± 0.029	A
^{135}Xe	0.019 ± 0.008	A	0.0886 ± 0.0046	[31]	0.755 ± 0.097	A	1.606 ± 0.284	A
^{136}Xe	0.957 ± 0.118	A	0.859 ± 0.158	A	3.735 ± 0.042	A	3.664 ± 0.415	A
^{137}Xe					3.637 ± 0.347	A	4.660 ± 0.165	A
^{138}Xe	3.072 ± 0.453	A	4.142 ± 0.168	A	4.165 ± 0.062	A	4.746 ± 0.899	A
^{139}Xe	5.421 ± 0.453	[26]	2.921 ± 0.007	A	(2.487)	A	(2.116)	A
			3.759 ± 0.040	[31]				
^{140}Xe	6.059 ± 0.422	[26]						
^{141}Xe	3.705 ± 0.353	[24]	2.638 ± 0.267	[31]				
^{142}Xe	2.227 ± 0.060	[24]						
^{143}Xe	0.722 ± 0.264	[24]	0.393 ± 0.014	[31]				
^{136}Cs	0.00017	[25]	0.00092	[31]	0.148 ± 0.036	A	0.173 ± 0.029	A
	± 0.000013							
^{137}Cs					0.557 ± 0.053	A	1.249 ± 0.378	A
^{138}Cs	0.0018 ± 0.0002	A	0.058 ± 0.042	[32]	1.343 ± 0.103	A	2.096 ± 0.208	A
^{139}Cs	0.355 ± 0.069	A	0.340 ± 0.057	[32]	2.588 ± 0.364	A	3.181 ± 0.035	A
^{140}Cs	1.145 ± 0.533	[26]	0.801 ± 0.058	A	2.786 ± 0.036	A	3.309 ± 0.645	A
^{141}Cs	3.109 ± 0.311	A	1.720 ± 0.380	[31]				
^{142}Cs	3.787 ± 0.379	A	1.900 ± 0.030	[31]				
^{143}Cs			1.820 ± 0.450	[31]				
^{145}Cs			0.510 ± 0.110	[31]				
^{146}Cs			0.112 ± 0.033	[31]				

Table 2. (Continued.)

Nuclide	^{233}Th*	Ref.	^{239}U*	Ref.	^{241}Pu*	Ref.	^{245}Cm*	Ref.
^{139}Ba					0.129 ± 0.012	A	0.816 ± 0.291	A
^{140}Ba	0.0494 ± 0.0074	A	0.1994 ± 0.0499	A	0.884 ± 0.254	A	1.700 ± 0.406	A
^{141}Ba	0.206 ± 0.025	A	0.490 ± 0.069	A	1.797 ± 0.287	A	2.914 ± 0.010	A
^{142}Ba	0.455 ± 0.046	A	1.565 ± 0.295	A	2.166 ± 0.216	A	3.125 ± 0.116	A
^{143}Ba	2.034 ± 0.125	A	1.985 ± 0.218	A				
^{144}Ba	$4.242 \pm 0 \pm 0.119$	A	2.390 ± 0.263	A	(2.063 ± 0.026)	A		
^{140}La					0.021 ± 0.005	A	0.075 ± 0.002	A
^{142}La	0.002 ± 0.001	A	0.150 ± 0.023	A	0.625 ± 0.298	A	0.969 ± 0.381	A
^{144}La	2.666 ± 0.571	A	0.592 ± 0.065	A	1.472 ± 0.034	A	1.932 ± 0.212	A
^{146}La	2.823 ± 0.091	A	(1.780 ± 0.196)	A	(1.349)	A		
^{144}Ce	(0.0079)	A	0.022 ± 0.005	A	0.119 ± 0.002	A	0.322 ± 0.027	A
^{146}Ce	0.890 ± 0.098	A	0.353 ± 0.101	A	0.951 ± 0.172	A	1.452 ± 0.138	A
^{148}Ce	1.254 ± 0.150	A	0.986 ± 0.127	A	1.004 ± 0.050	A	1.330 ± 0.017	A
^{146}Pr	0.026 ± 0.008	A	0.007 ± 0.003	A	0.077 ± 0.031	A	0.191 ± 0.078	A
^{148}Pr	0.181 ± 0.025	A	0.105 ± 0.015	A	0.714 ± 0.035	A	0.792 ± 0.047	A

A: present work.

Table 3. Isobaric dispersion parameter (σ_Z) and most probable charge (Z_P) of isobaric yields in ^{233}Th*, ^{239}U*, ^{241}Pu* and ^{245}Cm*. The σ_Z in parentheses is the assumed value as mentioned in the text.

Mass	^{233}Th*		^{239}U*		^{241}Pu*		^{245}Cm*	
No	σ_Z	Z_P	σ_Z	Z_P	σ_Z	Z_P	σ_Z	Z_P
128	(0.36)	49.55 ± 0.02	(0.40)	49.60 ± 0.10	(0.40)	50.20 ± 0.08	(0.45)	50.44 ± 0.10
129	–	–	–	–	(0.45)	50.54 ± 0.10	(0.48)	50.80 ± 0.10
130	(0.48)	50.10 ± 0.08	0.53	50.18 ± 0.10	0.47	50.78 ± 0.12	0.52	51.15 ± 0.15
131	0.55	50.40 ± 0.15	0.60	50.50 ± 0.15	0.56	51.16 ± 0.06	(0.62)	51.48 ± 0.13
132	0.52	50.68 ± 0.25	0.57	50.85 ± 0.12	0.52	51.50 ± 0.05	0.63	51.80 ± 0.15
133	0.45	51.35 ± 0.10	0.60	51.30 ± 0.05	0.60	51.86 ± 0.09	0.68	52.20 ± 0.12
134	(0.38)	51.80 ± 0.05	(0.45)	51.80 ± 0.05	(0.50)	52.30 ± 0.05	(0.57)	52.60 ± 0.15
135	0.54	51.96 ± 0.09	(0.56)	52.28 ± 0.04	(0.56)	52.76 ± 0.15	(0.60)	53.10 ± 0.13
136	0.36	53.00 ± 0.15	0.45	52.75 ± 0.05	0.45	53.45 ± 0.05	0.55	53.60 ± 0.05
137	–	–	–	–	(0.60)	53.70 ± 0.15	(0.60)	53.95 ± 0.07
138	(0.47)	53.30 ± 0.10	(0.47)	53.30 ± 0.10	(0.55)	54.00 ± 0.03	(0.60)	54.20 ± 0.08
139	(0.62)	53.50 ± 0.02	0.55	53.60 ± 0.07	(0.63)	54.24 ± 0.15	(0.63)	54.65 ± 0.12
140	0.60	53.95 ± 0.15	0.60	53.90 ± 0.05	0.63	54.80 ± 0.15	0.63	55.16 ± 0.07
141	0.57	54.43 ± 0.10	0.60	54.48 ± 0.10	(0.62)	55.35 ± 0.10	(0.62)	55.60 ± 0.15
142	0.54	55.05 ± 0.03	0.62	55.10 ± 0.10	(0.62)	55.60 ± 0.13	(0.60)	56.00 ± 0.15
143	(0.60)	55.22 ± 0.09	0.65	55.43 ± 0.15	–	–	–	–
144	(0.57)	55.70 ± 0.25	0.62	55.72 ± 0.04	(0.62)	56.30 ± 0.10	(0.65)	56.60 ± 0.10
146	(0.57)	56.80 ± 0.25	(0.60)	56.68 ± 0.08	(0.60)	57.30 ± 0.15	(0.62)	57.50 ± 0.05
148	(0.50)	57.50 ± 0.30	(0.57)	57.53 ± 0.15	(0.60)	58.10 ± 0.10	(0.62)	58.30 ± 0.15

$\mathrm{EOF}^{a(Z)}$ is the even-odd factor with $a(Z) = +1$ for even-Z nuclides and -1 for odd-Z nuclides.

From the above expression it is evident that, for the determination of Z_P, σ_Z and $\mathrm{EOF}^{a(Z)}$ it is essential to have at least three FCY values in a given isobaric chain. It can be seen from table 1 that FCY values of three isobars are not available for any mass chains in the fast-neutron–induced fission of ^{232}Th, ^{238}U, ^{240}Pu and ^{244}Cm. However, FCY values of at least two isobars are available for 8 mass chains in ^{232}Th(n_f,f), for 11 mass chains in ^{238}U(n_f,f), for 7 mass chains in ^{240}Pu(n_f,f) and for 7 mass chains in ^{244}Cm(n_f,f) systems, respectively. Accordingly the Z_P and σ_Z for these mass chains in the above-mentioned systems are obtained without correcting for the odd-even effects and are given in table 3. The even-odd effects were not considered to examine their effects on σ_Z and Z_P values. From the σ_Z values, the average width parameter of the isobaric yield distribution ($\langle\sigma_Z\rangle$) of the fissioning systems are also obtained. For isobaric chains, where the FCY value of only one isobar is available, the most probable charge (Z_P) has been evaluated using the σ_Z for the same mass of nearby fissioning systems having similar fissility parameter and are given in parentheses. For example the σ_Z for a particular mass chain in the fissioning systems ^{233}Th*, ^{239}U*, ^{241}Pu* and ^{245}Cm* were assumed to be the same as in the case of ^{230}Th* [21], ^{234,236}U* [39],

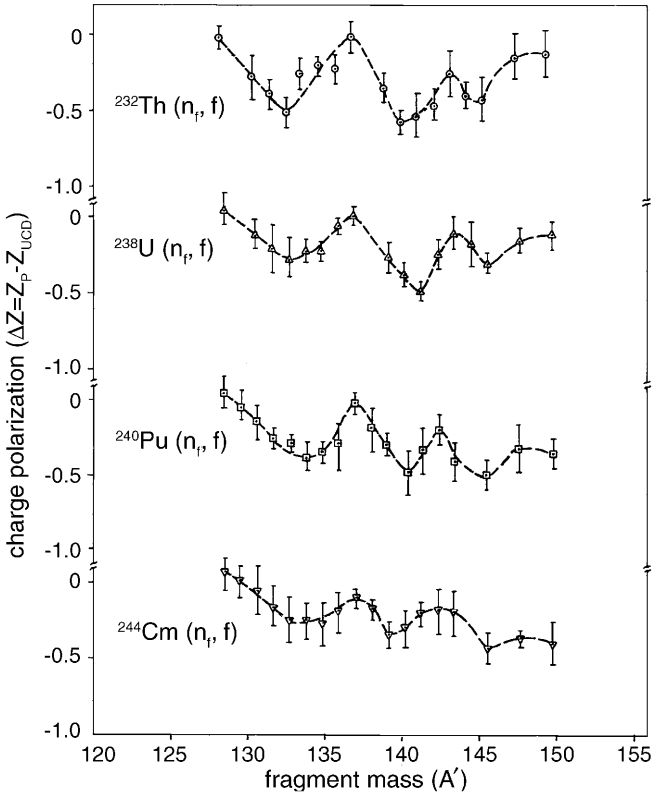

Fig. 1. The plot of charge polarization ($\Delta Z = Z_{\rm P} - Z_{\rm UCD}$) as a function of the fragment mass in fast-neutron–induced fission of ^{232}Th, ^{238}U, ^{240}Pu and ^{244}Cm.

^{240,242}Pu* [21,39] and ^{246}Cm* [21], respectively. The $Z_{\rm P}$ values thus obtained are given in table 3. The $Z_{\rm P}$ values are compared with the $Z_{\rm UCD}$ values expected from the unchanged charge density distribution to deduce the charge polarization ($\Delta Z = Z_{\rm P} - Z_{\rm UCD}$). The $Z_{\rm UCD}$ values for mass A are obtained using the equation

$$Z_{\rm UCD} = (Z_{\rm F}/A_{\rm F}) \times (A + \nu_A)\,, \qquad (2)$$

where $Z_{\rm F}$ and $A_{\rm F}$ are charge and mass of the fissioning system, respectively. ν_A is the number of neutrons emitted by the corresponding fission fragment and is evaluated according to the method of Erten and Aras [48]. Accordingly ν_A for the heavy and light fission product mass is given as

$$\nu_{\rm H} = 0.531\overline{\nu} + 0.062(A_{\rm H} - 143)\,, \qquad (3a)$$

$$\nu_{\rm L} = 0.531\overline{\nu} + 0.062(A_{\rm L} + 143 - A_{\rm F})\,, \qquad (3b)$$

where $\bar{\nu}$ is the average number of neutrons emitted during the fission process. It is taken as 2.35 for ^{233}Th* [54, 56], 2.790 for ^{239}U*, [54], 2.937 for ^{241}Pu* [54], respectively. In the case of ^{245}Cm* the average neutron number is not given in refs. [54,56]. So it is evaluated to be 3.857 by comparing the excitation energy and average neutron number with that of thermal-neutron–induced fission of ^{245}Cm [54]. This in turn is based on the comparison of the neutron emission trends in the thermal- and fast-neutron–induced fission of Th, U and Pu isotopes. The ΔZ values obtained as a function of the fragment mass in the fast-neutron–induced fission of ^{232}Th, ^{238}U, ^{240}Pu and ^{244}Cm are plotted in fig. 1.

3.1.2 Isotopic yield distribution

In the isotopic yield distribution the independent yields of isotopes for an element follows a Gaussian distribution [39]:

$$IY = \frac{Y_Z EOF^{b(N)}}{\sqrt{2\pi\sigma_A^2}} \int_{A-0.5}^{A+0.5} \exp[-(A - A_{\rm P})^2/2\sigma_A^2]{\rm d}A\,, \qquad (4)$$

where $A_{\rm P}$ is the most probable mass and σ_A is the isotopic dispersion parameter. Y_Z is the elemental yield and EOF$^{b(N)}$ is the even-odd factor with $b(N) = +1$ for even-N nuclides and -1 for odd-N nuclides.

It is evident from the above expression that for the determination of $A_{\rm P}$, σ_A, Y_Z and EOF$^{b(N)}$ it essential to have independent yields of at least four isotopes of an element. It can be seen from table 2 that independent yields of three or more isotopes of the elements Sb, Te, I, Xe, Cs, Ba, La and Ce are available in the fissioning systems ^{233}Th*, ^{239}U*, ^{241}Pu* and ^{245}Cm*. From these yields the most probable mass ($A_{\rm P}$), isotopic dispersion parameter (σ_A) and elemental yields (Y_Z) for the above elements are obtained using a non-linear least-square fit [21] without considering the even-odd effect of neutron and are given in tables 4-6.

4 Discussion

It can be seen from tables 1 and 2 that the fractional cumulative yields and independent yields of different fission products determined in the present work in the fast-neutron–induced fission of ^{232}Th and ^{238}U are in good agreement with the literature data [24–33]. However, in the fast-neutron–induced fission of ^{240}Pu and ^{244}Cm the data obtained in the present work are determined for the first time.

4.1 Charge distribution parameters and their relevance to nuclear structure effect and descent dynamics

Table 3 shows that in the fissioning systems ^{233}Th*, ^{239}U*, ^{241}Pu* and ^{245}Cm* the charge dispersion parameter σ_Z is decreasing with the approach of $Z_{\rm P} = 50 (A = 128$–$130)$ and $N_{\rm P} = 82 (A = 134$–$136)$ which indicates the effect of shell closure proximity on σ_Z. On the other hand, the oscillating nature of σ_Z as a function of the fragment mass [11–20,36,57] indicates the presence of the odd-even effect. The odd-even effect is also felt on $Z_{\rm P}$ through the oscillating nature of ΔZ with an interval of five mass units [16], as shown in fig. 1 for the fissioning systems ^{233}Th*, ^{239}U*, ^{241}Pu* and ^{245}Cm*. Apart from the oscillating nature, a systematic decrease of ΔZ with the approach of symmetric split was observed for the above four

Table 4. Elemental yields of various elements in ^{233}Th*, ^{239}U*, 241Pu* and ^{245}Cm*.

Element	^{233}Th*	Ref.	^{239}U*	Ref.	^{241}Pu*	Ref.	^{245}Cm*	Ref.
Sn	4.50 ± 0.84	A	4.86 ± 0.58	A	2.13 ± 0.08	A	2.52 ± 0.36	A
Sb	6.32 ± 0.68	A	10.73 ± 0.63	A	10.30 ± 1.71	A	6.42 ± 0.98	A
Te	12.18 ± 0.37	A	16.92 ± 1.14	A	19.62 ± 3.44	A	16.16 ± 0.76	A
I	6.01 ± 0.18	A	12.76 ± 0.12	A	12.22 ± 1.83	A	16.03 ± 3.32	A
Xe	22.87 ± 1.23	A	22.53 ± 1.86	A	16.40 ± 2.92	A	18.50 ± 2.52	A
Cs	11.11 ± 1.00	A	8.45 ± 0.31	A	9.89 ± 0.66	A	14.26 ± 1.68	A
Ba	15.26 ± 0.29	A	10.03 ± 2.09	A	11.61 ± 1.13	A	12.59 ± 1.15	A
La	8.87 ± 0.10	A	5.90 ± 0.02	A	7.84 ± 0.75	A	7.59 ± 0.51	A
Ce	4.41 ± 0.07	A	4.04 ± 0.17	A	4.38 ± 0.16	A	6.60 ± 0.29	A
Pr	1.20 ± 0.18	A	0.65 ± 0.14	A	3.97 ± 0.46	A	2.96 ± 0.09	A

A: present work.

Table 5. Most probable mass ($A_{\rm P}$) of isotopic yields in ^{233}Th*, ^{239}U*, ^{241}Pu* and ^{245}Cm*.

Element	^{233}Th*	Ref.	^{239}U*	Ref.	^{241}Pu*	Ref.	^{245}Cm*	Ref.
Sn	131.7 ± 0.23	A	131.2 ± 0.16	A	129.2 ± 0.06	A	128.6 ± 0.19	A
Sb	133.4 ± 0.15	A	132.4 ± 0.09	A	131.7 ± 0.30	A	131.6 ± 0.27	A
Te	134.6 ± 0.04	A	134.7 ± 0.06	A	134.2 ± 0.79	A	133.5 ± 0.09	A
I	136.6 ± 0.04	A	136.3 ± 0.02	A	135.0 ± 0.21	A	135.8 ± 0.40	A
Xe	139.7 ± 0.10	A	138.7 ± 0.21	A	137.4 ± 0.28	A	137.3 ± 0.21	A
Cs	141.8 ± 0.12	A	142.1 ± 0.07	A	139.7 ± 0.08	A	139.6 ± 0.24	A
Ba	144.3 ± 0.50	A	143.8 ± 0.43	A	142.8 ± 0.21	A	141.7 ± 0.16	A
La	145.9 ± 0.01	A	146.0 ± 0.09	A	144.8 ± 0.22	A	143.9 ± 0.16	A
Ce	147.2 ± 0.03	A	148.4 ± 0.08	A	147.1 ± 0.05	A	146.9 ± 0.07	A
Pr	149.6 ± 0.29	A	150.1 ± 0.38	A	148.6 ± 0.31	A	148.4 ± 0.04	A

A: present work.

Table 6. Isotopic dispersion parameter (σ_A) in ^{233}Th*, ^{239}U*, ^{241}Pu* and ^{245}Cm*.

Element	^{233}Th*	Ref.	^{239}U*	Ref.	^{241}Pu*	Ref.	^{245}Cm*	Ref.
Sn	1.17 ± 0.25	A	1.51 ± 0.22	A	1.54 ± 0.08	A	2.07 ± 0.32	A
Sb	1.27 ± 0.16	A	1.43 ± 0.10	A	1.98 ± 0.39	A	2.40 ± 0.33	A
Te	1.11 ± 0.04	A	1.20 ± 0.05	A	2.08 ± 0.50	A	1.90 ± 0.12	A
I	1.15 ± 0.02	A	1.36 ± 0.09	A	1.25 ± 0.24	A	1.65 ± 0.31	A
Xe	1.59 ± 0.11	A	1.96 ± 0.19	A	1.55 ± 0.35	A	1.68 ± 0.22	A
Cs	1.18 ± 0.11	A	1.71 ± 0.07	A	1.43 ± 0.09	A	1.72 ± 0.20	A
Ba	1.27 ± 0.23	A	1.73 ± 0.33	A	1.90 ± 0.24	A	1.62 ± 0.14	A
La	1.07 ± 0.05	A	1.35 ± 0.05	A	1.97 ± 0.23	A	1.60 ± 0.12	A
Ce	1.13 ± 0.04	A	1.63 ± 0.05	A	1.47 ± 0.06	A	1.63 ± 0.08	A
Pr	1.70 ± 0.16	A	1.67 ± 0.16	A	1.91 ± 0.26	A	1.64 ± 0.05	A

A: present work.

fissioning systems which is characteristics of low-energy fission as mentioned by Armbruster *et al.* [1] and shown by Wilkins *et al.* [57] in their static scission point model. The $\Delta Z_{\rm MPE}$ value based on the minimum potential energy model also shows a decreasing trend with the approach of symmetric split [21,45] in several fissioning systems confirming the above facts. From fig. 1 the slopes of charge polarization with mass asymmetry $[\delta(\Delta Z)/\delta A']$ are also obtained for the above four fissioning systems using the equation suggested by Wahl [39]

$$\Delta Z(A') = (A' - 140)\frac{\delta(\Delta Z)}{\delta A'} + \Delta Z(A' = 140)\,, \qquad (5)$$

where $\Delta Z(A' = 140)$ is the charge polarization for the fragment mass 140. These values of $\delta(Z)/\delta A'$ from the present work along with the literature data [21,24,39,46] for twelve fissioning systems are given in table 7. The $\delta(\Delta Z/\delta A')$ value in ^{233}Th* from the present work is in good agreement with the value determined earlier [24], whereas in the case of ^{239}U*, ^{241}Pu* and ^{245}Cm* they are determined for the first time. The $\delta(\Delta Z)/\delta A'$ values from table 7 are plotted in fig. 2 as a function of the fissility parameter ($Z_{\rm F}^2/A_{\rm F}$). From fig. 2 a systematic increase of $[\delta(\Delta Z/\delta A')]$ with increase in $Z_{\rm F}^2/A_{\rm F}$ is observed except in ^{252}Cf(SF). As is shown by Nix [58] the saddle point shapes

Table 7. Average number of neutrons, charge distribution parameters, % odd-even effect and intrinsic excitation energy in different fissioning systems.

A_F	$\bar{\nu}$	$\delta(\Delta Z)/\delta A'$	$\langle\sigma_Z\rangle$	$\delta_P(\%)$	$\delta_N(\%)$	E_{diss} MeV	$E^* - B_0$ MeV
$^{230}Th^*$	$2.080^{(a)}$	$-0.005 \pm 0.004^{(k)}$	$0.51 \pm 0.08^{(k)}$	$41.2 \pm 1.0^{(o)}$	$1.95 \pm 0.5^{(p)}$	3.55 ± 0.10	0.29
				$40.0 \pm 4.0^{(p)}$		3.67 ± 0.38	
				$35.0 \pm 5.0^{(q)}$		4.20 ± 0.53	
				$35.3 \pm 6.1^{(k)}$		4.17 ± 0.64	
$^{232}Th^*$	–	–	–	$30.0 \pm 2.0^{(v)}$	–	4.82 ± 0.26	-0.20
$^{233}Th^*$	$2.350^{(b)}$	$-0.004 \pm 0.004^{(l)}$	$0.52 \pm 0.02^{(b)}$	$30.0 \pm 12.0^{(r)}$	–	4.82 ± 1.35	0.04
		$-0.005 \pm 0.003^{(x)}$	$0.52 \pm 0.08^{(x)}$	$26.0 \pm 2.0^{(l)}$	5.39 ± 0.30		
				$27.7 \pm 2.2^{(x)}$		5.13 ± 0.31	
$^{233}U^*$	$2.800^{(c)}$	–	–	$21.0 \pm 3.0^{(p)}$	–	6.24 ± 0.53	-0.05
				$24.6 \pm 3.0^{(c)}$		5.61 ± 0.46	
$^{234}U^*$	$2.495^{(d)}$	$-0.015 \pm 0.002^{(i)}$	$0.56 \pm 0.01^{(i)}$	$21.0 \pm 7.5^{(r)}$	$5.4 \pm 1.5^{(s)}$	6.24 ± 1.22	1.34
				$22.1 \pm 2.1^{(s)}$		6.04 ± 0.36	
$^{236}U^*$	$2.422^{(d)}$	$-0.008 \pm 0.001^{(i)}$	$0.53 \pm 0.01^{(i)}$	$22.0 \pm 5.4r$	$5.4 \pm 0.7^{(t)}$	6.06 ± 0.88	1.02
				$23.7 \pm 0.7^{(t)}$		5.76 ± 0.12	
$^{238}U^*$	–	–	–	$29.0 \pm 2.0^{(w)}$	$3.0 \pm 2.0^{(w)}$	4.95 ± 0.27	-0.04
$^{239}U^*$	$2.790^{(d)}$	$-0.008 \pm 0.003^{(x)}$	$0.55 \pm 0.05^{(n)}$	$20.0 \pm 11.0^{(r)}$	–	6.44 ± 1.75	0.55
	$2.650^{(b)}$		$0.55 \pm 0.07^{(x)}$	$20.5 \pm 3.3^{(x)}$		6.34 ± 0.60	
$^{239}Pu^*$	$2.892^{(e)}$	–	–	$14.0 \pm 0.3^{(f)}$	–	7.86 ± 0.08	-0.05
$^{240}Pu^*$	$2.880^{(d)}$	$-0.015 \pm 0.002^{(i)}$	$0.56 \pm 0.01^{(i)}$	$11.6 \pm 0.6^{(u)}$	$6.4 \pm 0.7^{(u)}$	8.62 ± 0.20	1.46
				$11.8 \pm 9.0^{(r)}$		8.55 ± 2.27	
$^{241}Pu^*$	$2.937^{(d)}$	$-0.014 \pm 0.003^{(x)}$	$0.56 \pm 0.07^{(x)}$	$10.7 \pm 5.6^{(x)}$	–	8.94 ± 1.68	1.64
	$3.260^{(b)}$						
$^{242}Pu^*$	$2.868^{(d)}$	$-0.015 \pm 0.005^{(k)}$	$0.56 \pm 0.06^{(k)}$	$12.2 \pm 5.4^{(k)}$	–	8.41 ± 1.47	1.21
				$10.0 \pm 1.5^{(j)}$		9.21 ± 0.56	
$^{245}Cm^*$	$3.867^{(d)}$	$-0.018 \pm 0.003^{(x)}$	$0.60 \pm 0.07^{(x)}$	$8.8 \pm 4.7^{(x)}$		9.72 ± 1.71	2.42
$^{246}Cm^*$	$3.825^{(d)}$	$-0.019 \pm 0.004^{(k)}$	$0.60 \pm 0.07^{(k)}$	$9.6 \pm 2.7^{(k)}$	–	9.37 ± 0.99	2.16
	$3.832^{(f)}$		$0.60^{(g)}$				
$^{250}Cf^*$	$4.096^{(g)}$	$-0.025 \pm 0.002^{(m)}$	$0.63 \pm 0.02^{(m)}$	$4.6 \pm 0.7^{(h)}$	$9.5 \pm 0.7^{(h)}$	12.32 ± 0.57	3.02
	$4.400^{(h)}$		$0.63 \pm 0.05^{(g)}$	$7.0 \pm 5.0^{(m)}$		10.64 ± 2.16	
$^{252}C^{(f)}$	$3.820^{(i)}$	$-0.015 \pm 0.006^{(k)}$	$0.59 \pm 0.06^{(k)}$	$12.0 \pm 2.0^{(q)}$	–	8.48 ± 0.62	-3.60
	$3.765^{(d)}$	$-0.015 \pm 0.006^{(i)}$	$0.59 \pm 0.02^{(i)}$	$10.8 \pm 2.2^{(k)}$		8.90 ± 0.74	

([a]) Ref. [23]. ([b]) Ref. [56]. ([c]) Ref. [35]. ([d]) Ref. [54]. ([e]) Ref. [41]. ([f]) Ref. [42]. ([g]) Ref. [44], ([h]) Ref. [15]. ([i]) Ref. [39]. ([j]) Ref. [20]. ([k]) Ref. [21]. ([l]) Ref. [24], ([m]) Ref. [46]. ([n]) Ref. [32]. ([o]) Ref. [17]. ([p]) Refs. [17,18]. ([q]) Refs. [9,10]. ([r]) Ref. [26]. ([s]) Ref. [14]. ([t]) Ref. [12]. ([u]) Ref. [13]. ([v]) Ref. [28]. ([w]) Ref. [29]. ([x]) Present work.

of fissioning nuclei become more compact with increase in the fissility parameter and the distance from the saddle to scission also increases with Z_F^2/A_F. Thus, to reach the scission shape, more time is necessary with increase in Z_F^2/A_F. However, this is valid up to the formation of the neck [15–17]. Once the neck is formed, its snapping may have its own dynamics [15–17,21,59]. The average charge dispersion parameter ($\langle\sigma_Z\rangle$) is the best parameter to give some important information about the last part of the scission, *i.e.* at the point of the neck rupture. The average charge dispersion parameter ($\langle\sigma_Z\rangle$) for the fissioning systems $^{233}Th^*$, $^{239}U^*$, $^{241}Pu^*$ and $^{246}Cm^*$ from the present work as well as for the other fissioning systems from radiochemical methods [21,39,42,46] are given in table 7. The $\langle\sigma_Z\rangle$ value in the fast-neutron–induced fission of ^{232}Th and ^{238}U from refs. [24,32] are also given in the same table and are seen to be in agreement with the value from the present work. The $\langle\sigma_Z\rangle$ value in the fast-neutron–induced fission of ^{240}Pu and ^{244}Cm are determined for the first time. The variance ($\langle\sigma_Z^2\rangle$) is plotted in fig. 3 as a function of Z_F^2/A_F. From fig. 3 a systematic increase of $\langle\sigma_Z^2\rangle$ with increase in Z_F^2/A_F was observed except in ^{252}Cf(SF). According to Asghar *et al.* [60] in the process of charge equilibration at a fixed mass value, the N/Z mode is commonly described by a harmonic oscillator having a phonon energy $\hbar\omega$. This oscillator is coupled to the intrinsic degrees of freedom. Under these conditions the variance $\langle\sigma_Z^2\rangle$ observed in the low-energy fission is the result of zero point oscillation and is given by [16,21,61]

$$\langle\sigma_Z^2\rangle = \frac{\hbar}{2M\omega} = \frac{3\hbar}{4\pi\omega}\,\frac{1}{r_0^3 m_0}\,\frac{Z_F N_F}{A_F^2}\,c \qquad (6)$$

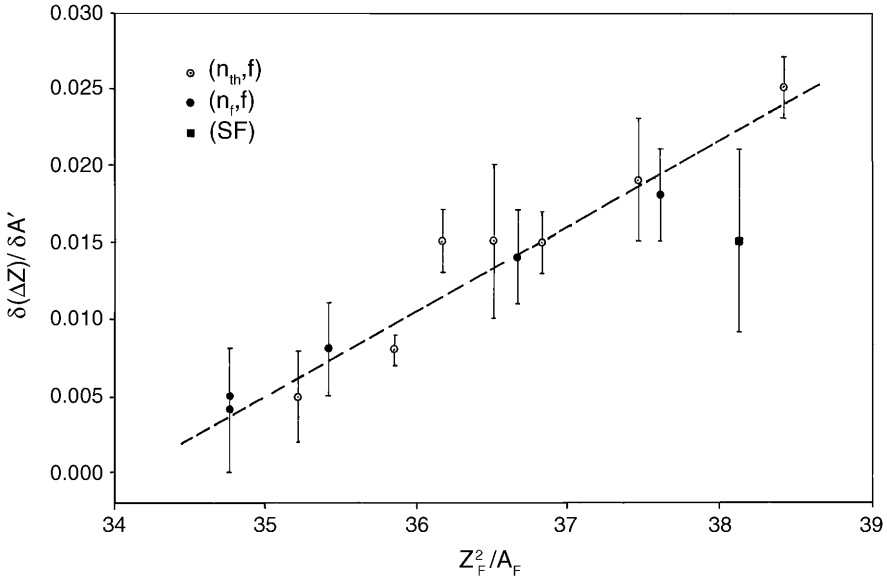

Fig. 2. The plot of the slope of charge polarization $[\delta(\Delta Z)/\delta A']$ as a function of the fissility parameter $(Z_{\rm F}^2/A_{\rm F})$.

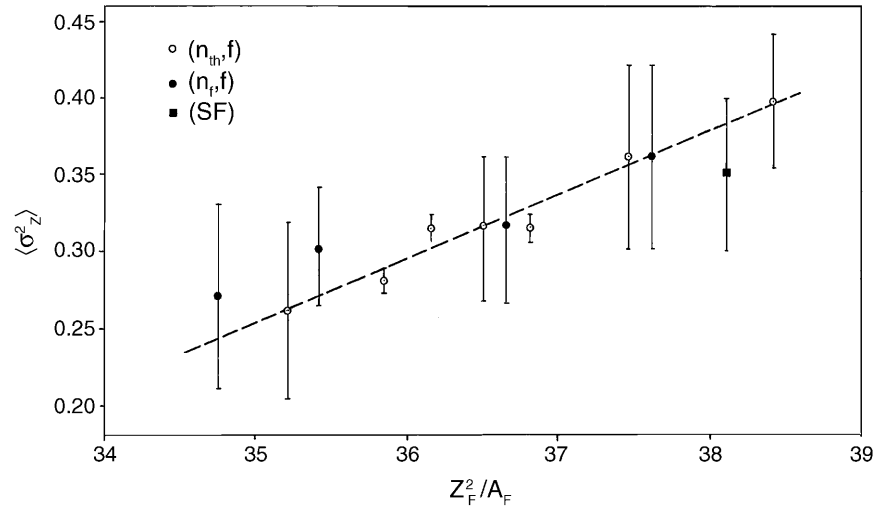

Fig. 3. The plot of average isobaric charge variance $(\langle\sigma_Z^2\rangle)$ as a function of the fissility parameter $(Z_{\rm F}^2/A_{\rm F})$.

where M is the inertia parameter of the N/Z mode [62]. r_0 and m_0 are the nuclear radius and mass. c is the neck radius between the two nascent fragments.

From the above equation it is clear that $\langle\sigma_Z^2\rangle$ is independent of the temperature, *i.e.* excitation energy [12–17, 21]. The near identical values of $\langle\sigma_Z\rangle$ for both thermal- and fast-neutron–induced fission of the same even-Z actinides with odd and even mass (*e.g.*, ^{229}Th and ^{232}Th, ^{233,235}U and ^{238}U, ^{239,241}Pu and ^{240}Pu, ^{244}Cm and ^{245}Cm) support this fact. Further, from the above equation it can be seen that in the static approach, $\langle\sigma_Z^2\rangle$ has practically the same value for $90 < Z_{\rm F} < 98$ which is in contradiction with the experimental results. The dependence of $\langle\sigma_Z^2\rangle$ on $Z_{\rm F}$ should have a dynamical origin through the change of neck radius c with time. The numerical solution of the time-dependent Schrodinger equation for such a variable-mass harmonic oscillator has been solved by Nifenecker [59], who found the linear correlation of $\langle\sigma_Z^2\rangle$ with $\mathrm{d}c/\mathrm{d}t$. From the above discussion it is clear that the time of descent from saddle to the point of formation of the neck gets slower with increasing $Z_{\rm F}^2/A_{\rm F}$. Once the neck is formed its snapping gets faster with increasing $Z_{\rm F}^2/A_{\rm F}$.

4.2 Odd-even effect and its correlation with intrinsic excitation energy and charge variance

The odd-even effect in the elemental yields for the fissioning systems ^{233}Th*, ^{239}U*, ^{241}Pu* and ^{245}Cm based on radiochemical measurements was evaluated by the normalized difference between the total yields for even and odd charge splits $Y_{\rm e}$ and $Y_{\rm o}$, respectively:

$$\delta_{\rm p}(\%) = \frac{\Sigma Y_{\rm e} - \Sigma Y_{\rm o}}{\Sigma Y_{\rm e} + \Sigma Y_{\rm o}} \times 100\,. \qquad (7)$$

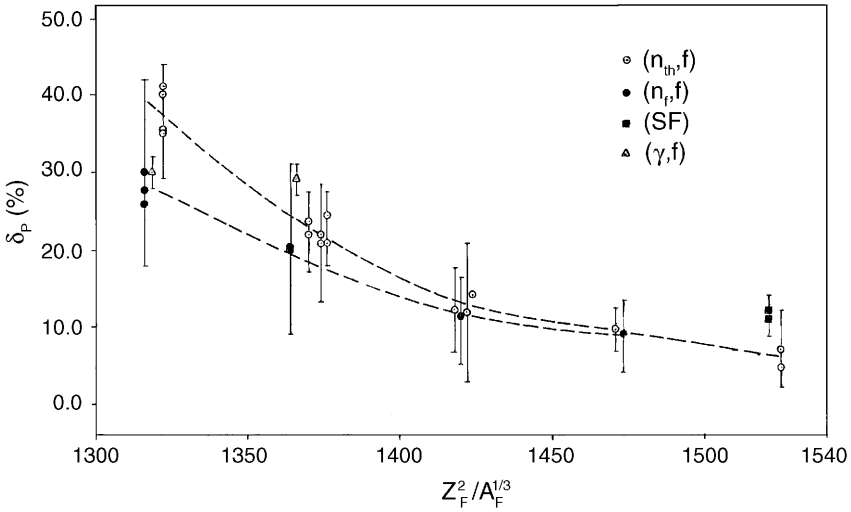

Fig. 4. The plot of the amplitude of the proton odd-even effect (δ_p) as a function of the Coulomb parameter ($Z_F^2/A_F^{1/3}$).

These data along with the literature data for other neutron-induced even-Z fissioning systems obtained in radiochemical [21,26–29,35,38–41,45] and physical measurements [8–20] are given in table 7. Data for sixteen fissioning systems have been given which includes γ-ray, thermal- and fast-neutron–induced fissioning systems as well as spontaneous-fissioning systems. The odd-even effect in ^{233}Th* and ^{239}U* determined from the present work are in good agreement with the value determined by Amiel and Feldstein [26]. The odd-even effect in ^{241}Pu* and ^{245}Cm* from the present work has been determined radiochemically for the first time. The proton odd-even effect (δ_p) for sixteen fissioning systems from table 7 are plotted in fig. 4 as a function of the Coulomb parameter ($Z_C = Z_F^2/A_F^{1/3}$). Leaving behind the data of ^{252}Cf(SF) the data of thermal- and fast-neutron–induced fission of actinides are represented by two separate curves which are very well represented by the empirical relation $\delta_p = a[\exp(-bZ_C)]$ with different a and b values. For thermal-neutron–induced fissioning systems, the empirical relation has the value of constant $a = \exp(15.9)$ and $b = 0.00932$. On the other hand, in the fast-neutron–induced fission of ^{232}Th, ^{238}U, ^{240}Pu and ^{244}Cm the odd-even effects are slightly lower if one ignores the error bar and can be represented by the similar empirical relation with the constant $a = \exp(13.6)$ and $b = 0.00779$. The exponential dependence of the proton odd-even effect on Coulomb parameter can be explained from the point of view of its dependence on the intrinsic excitation energy [15–17,21,63]. However, the deviation of δ_p for ^{252}Cf(SF) may be due to a deficit of excitation energy compared to the thermal-neutron–induced fissioning system. Comparing the mass yield data in ^{240}Pu(SF) and ^{239}Pu(n_{th},f) Schillebeeckx *et al.* [64] indicated that in neutron-induced fission increase in excitation energy mainly results in increase in intrinsic excitation energy. Thus the lower intrinsic excitation energy in spontaneous fission compared to thermal-neutron–induced fission results in higher odd-even effect in the former than the latter. Similarly in fast-neutron–induced fission, the availability of higher intrinsic excitation energy might be reducing the odd-even effect compared to the thermal-neutron–induced fissioning system. Otherwise, it can be seen from table 7 that the excitation energy above the second saddle ($E^* - V_B$) in the thermal-neutron–induced fission of even-odd actinides (^{229}Th, ^{233,235}U, ^{239,241}Pu, ^{245}Cm, ^{249}Cf) and in the fast-neutron–induced fission of even-even actinides (^{232}Th, ^{238}U, ^{240}Pu, ^{244}Cm) are just sufficient to overcome the second saddle. This is supported from the drastic change of the odd-even effect of 8% and 5% in the fast (1.9 MeV) and the 3 MeV neutron-induced fission of ^{235}U [40] compared to 25% in its thermal-neutron–induced fission [38]. The decrease of the odd-even effect of 18% in the 3 MeV neutron-induced fission of ^{238}U [34] compared to 20% in its fast (1.9 MeV) neutron-induced fission [26] further supports this fact. Similarly, in the γ-ray–induced fission of ^{238}U [29] the odd-even effect of 20% above the saddle point excitation energy increases to 29% below the barrier excitation energy. However, the odd-even effect of 30% below the barrier excitation energy in the γ-ray–induced fission of ^{232}Th [28] is not clear. According to the above justification the odd-even effect of 30% should be for excitation energy above the barrier.

This is possible only if one considers the triple-hump fission barrier in ^{232}Th [65] where it has been shown that asymmetric fission barrier is lower than the symmetric fission barrier. From these observations it is clear that the excitation energy is the deciding factor for the odd-even effect. The dependence of the odd-even effect both on excitation energy at the saddle and on the dissipated energy on the path from saddle to scission is very clearly shown in the statistical model of Rejmund *et al.* [63]. However, it is still not known where the q-p excitation occur. From table 7 it can be seen that the excitation energy above the second saddle ($E^* - V_B$) in the thermal- and fast-neutron–induced fission of the different fissioning systems is not sufficient to excite q-p at the saddle point except in the case of the fissioning systems ^{245,246}Cm* and ^{250}Cf*. In the thermal-neutron–induced fissioning systems ^{233}U*

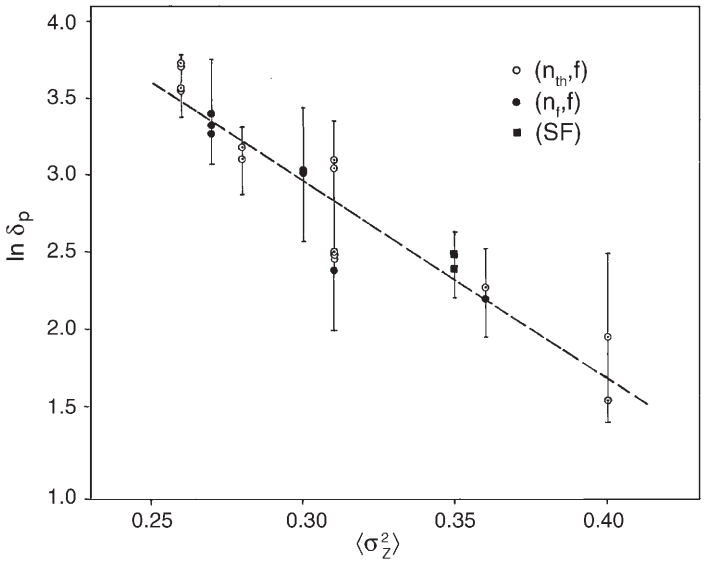

Fig. 5. The plot of $\ln \delta_{\rm p}$ *vs.* average isobaric charge variance ($\langle \sigma_Z^2 \rangle$) in different fissioning systems.

and ^{239}Pu* as well as below the barrier γ-ray–induced fissioning systems ^{232}Th* and ^{238}U*, the $E^* - V_{\rm B}$ values are negligible or negative. On the other hand, the spontaneous-fissioning system ^{252}Cf is an excitation energy deficit system. Therefore, the motion from saddle to scission in the low-energy fission of even-Z spontaneous fissioning systems, below the barrier gamma-induced or neutron-induced fissioning systems should start in paired configuration. The experimental evidence that odd-Z fragments are produced in low-energy fission indicates that the q-p excitation and thus the proton pairs are broken in the deformed nucleus enroute to scission except in the fissioning systems ^{245,246}Cm* and ^{250}Cf* where the pair breaking may start at the second saddle point. Obviously the proton odd-even effect must reflect the number of broken pairs either at the start of the second saddle point or at the enroute to the scission point. In other words $\delta_{\rm p}$ can be considered as a probe for the intrinsic excitation energy ($E_{\rm diss}$). This can be calculated from the odd-even effect as prescribed by Nifenecker *et al.* [66] and used by others [28, 29, 63]:

$$E_{\rm diss} = -4 \ln \delta_{\rm p} \,. \tag{8}$$

$E_{\rm diss}$ is calculated for different fissioning systems using eq. (8) and is given in table 7. The $E_{\rm diss}$ value is seen to be increasing systematically with increase of the fissility parameter of the fissioning systems except for the spontaneous fission of ^{252}Cf and below the barrier excitation energy of ^{238}U(γ,f). This observation very clearly indicates the role of the excitation energy in the low-energy fission of actinides. However, it is not known when the collective energy is converted into nucleon excitation due to a loss of adiabaticity that is proportional to the deformation velocity [16, 67]. In other words, it is not clear whether the q-p excitation takes place in the path of saddle to scission or at the point of scission, *i.e.* during neck rupture. If the excitation occurs at scission, then the above estimate would appear to be an upper limit for dissipation during the descent alone. This $E_{\rm diss}$ has a linear correlation with the Coulomb parameter and is exponentially related to the odd-even effect. On the other hand, it has been shown earlier [16] that the variance ($\langle \sigma_Z^2 \rangle$) which increases linearly with the Coulomb parameter has a linear correlation with the necking velocity dc/dt. The final process of neck pinching is a non-adiabatic effect [15–17] and then it should have a correlation with the process involving the damping of collective energy into intrinsic excitation energy ($E_{\rm diss}$). In other words, $E_{\rm diss}$ should have a linear correlation with dc/dt which was clearly shown earlier [16]. Thus the experimentally obtained quantity $\langle \sigma_Z^2 \rangle$ should show a linear correlation with $\ln \delta_{\rm p}$. This is very well seen from fig. 5 including the point for fast-neutron–induced fission of ^{232}Th, ^{238}U, ^{240}Pu and ^{244}Cm and in particular for ^{252}Cf(SF). Due to non-availability of $\langle \sigma_Z \rangle$ in ^{238}U(γ,f) and ^{232}Th(γ,f) it is not possible to test this relation for the systems having below barrier excitation energy. However, the above observation clearly indicates that q-p excitation and snapping of neck occur non-adiabatically.

From the above discussions, the conclusions drawn are as follows:

i) In the fast-neutron–induced fission of ^{232}Th, ^{238}U, ^{240}Pu and ^{244}Cm the width parameter (σ_Z) is lower for $Z_{\rm P} = 50$ ($A = 128$–130) and $N_{\rm P} = 82$ ($A = 132$–136) indicating the effect of proximity of shell closure. On the other hand, the oscillating nature of σ_Z and ΔZ with fragment mass reflects the odd-even effect.

ii) Besides the oscillating nature, the ΔZ values systematically decrease with the approach of symmetric split. The slope of charge polarization with fragment mass $[\delta(\Delta Z)/\delta A']$ increases systematically with increasing the fissility parameter which is explained on the basis of the larger time taken by the higher fissioning system to reach the scission shape (*i.e.* up to the neck formation) due to a more compact saddle shape. On the other hand, the systematic increase of the charge

variance ($\langle\sigma_Z^2\rangle$) with Z_F^2/A_F is explained on the basis of zero-point oscillation in the charge equilibration mode and is thus related to the necking velocity (dc/dt). These two observations together indicate that the dynamics of descent from the saddle to the formation of the neck is slower with increasing Z_F^2/A_F and once the neck is formed it is faster with increasing Z_F^2/A_F.

iii) The odd-even effect in the fast-neutron–induced fission of ^{232}Th, ^{238}U, ^{240}Pu and ^{244}Cm decreases exponentially with the Coulomb parameter ($Z_F^2/A_F^{1/3}$) like the fissioning systems induced by the thermal neutron but follows a separate curve. This indicates that the intrinsic excitation energy increases with increase of $Z_F^2/A_F^{1/3}$ and it is slightly high for fast-neutron–induced fissioning systems. On the other hand, the correlation of $\ln\delta_p$ with $\langle\sigma_Z^2\rangle$ indicates that quasiparticle excitation and snapping of the neck occur non-adiabatically.

The authors wish to express their sincere gratitude to the instrumentation group of Radiochemistry Division for their assistance.

References

1. P. Armbruster, D. Hovestadt, H. Meister, H.J. Specht, Nucl. Phys. **54**, 586 (1964); K. Sistemich, P. Armbruster, J. Eidens, E. Roeckl, Nucl. Phys. **139**, 289 (1969).
2. E. Konecny, H. Opower, H. Gunther, H. Gobel, in *Proceedings of the First IAEA Symposium on Physics and Chemistry of Fission, Salzburg*, Vol. **I** (IAEA, Vienna, 1965) p. 401.
3. W. Reisdorf, J.P. Unik, H.C. Griffin, L.E. Glendenin, Nucl. Phys. A **177**, 337 (1971).
4. E. Cheifetz, J.B. Wilhelmy, R.C. Jared, S.G. Thompson, Phys. Rev. C **4**, 1913 (1971).
5. S.J. Balestrini, R. Decker, H. Wollnik, K.D. Wunsch, G. Jung, E. Koglin, G. Siegert, Phys. Rev. C **20**, 2244 (1979).
6. M. Shmid, Y. Nir-el, G. Engler, S. Amiel, J. Inog. Nucl. Chem. **43**, 867 (1981).
7. R. Brissot, J. Crancon, Ch.Ristori, J.P. Bocquet, A. Moussa, Nucl. Phys. A **282**, 109 (1977); **255**, 461 (1975).
8. M. Djebara, M. Asghar, J.P. Bocquet, R. Brissot, M. Maurel, H. Nifenecker, Ch. Ristori, Nucl. Phys. A **425**, 120 (1984).
9. G. Mariolopoulos, Ch. Hamelin, J. Blachot, J.P. Bocquet, R. Brissot, J. Crancon, H. Nifenecker, Ch. Ristori, Nucl. Phys. A **361**, 213 (1981).
10. T. Datta, P.K. Pujari, S.K. Das, B.S. Tomar, S.B. Manohar, A. Goswami, H. Naik, SatyaPrakash, *IAEA Symposium on Physics and Chemics of Fission, Gaussig, GDR, November, 1988*.
11. G. Siegert, H. Wollnik, J. Greif, R. Decker, G. Fiedler, B. Pfeiffer, Phys. Rev. C **14**, 1864 (1976).
12. W. Lang, H.G. Clerc, H. Wohlfarth, H. Schrader, K.H. Schmidt, Nucl. Phys. A **345**, 34 (1980); H.G. Clerc, W. Lang, W. Wohlfarth, K.H. Schmidt, H. Schrader, K.E. Pferdekamper, R. Jungmann, Z. Phys. A **274**, 203 (1975).
13. C. Schmitt, A. Guessous, J.P. Bocquet, H.G. Clerc, R. Brissot, D. Engelhardt, H.R. Faust, F. Gonnenwein, M. Mutterer, H. Nifenecker, J. Pannicke, Ch. Ristori, J.P. Theobald, Nucl. Phys. A **430**, 21 (1984).
14. U. Quade, K. Rudolph, S. Skorka, P. Armbruster, H.G. Clerc, W. Lang, M. Mutterer, C. Schmitt, J.P. Theobald, F. Gonnenwein, J. Pannicke, H. Schrader, G. Siegert, D. Engelhardt, Nucl. Phys. A **487**, 1 (1988).
15. M. Djebara, M. Asghar, J.P. Bocquet, R. Brissot, J. Crancon, Ch.Ristori, E. Aker, D. Engelhardt, J. Gindler, B.D. Wilkins, U. Quade, K. Rudolph, Nucl. Phys. A **496**, 346 (1989).
16. J.P. Bocquet, R. Brissot, Nucl. Phys. A **502**, 213 (1989).
17. J.P. Bocquet, R. Brissot, H.R. Faust, M. Fowler, J. Wilhelmy, M. Asghar, M. Djebara, Z. Phys. A **335**, 41 (1990).
18. N. Boucheneb, P. Geltenbort, M. Asghar, G. Barreau, T.P. Doan, F. Gonnenwein, B. Leroux, A. Oed, A. Sicre, Nucl. Phys. A **502**, 261 (1989).
19. N. Boucheneb, M. Asghar, G. Barreau, T.P. Doan, B. Leroux, A. Sicre, P. Gelterbort, A. Oed, Nucl. Phys. A **535**, 77 (1991).
20. P. Schillebeeckx, C. Wagemans, P. Geltenbort, F. Gonnenwein, A. Oed, Nucl. Phys. A **580**, 15 (1994).
21. H. Naik, S.P. Dange, R.J. Singh, S.B. Manohar, Nucl. Phys. A **612**, 143 (1997); H. Naik, S.P. Dange, R.J. Singh, Radiochim. Acta **83**, 109 (1998).
22. J.K. Dickens, J.W. McConnell, Phys. Rev. C **27**, 253 (1983); J.K. Dickens, J.W. McConnell, K.J. Northcutt, Nucl. Sci. Eng. **80**, 455 (1982).
23. M. Haddad, J. Crancon, G. Lhospice, M. Asghar, J. Blachot, Radiochim. Acta **42**, 165 (1987).
24. R. Hentzschel, H.O. Denschlag, Radiochim. Acta **50**, 1 (1990); Alok Srivastava, H.O. Denschlag, Radiochim. Acta **46**, 17 (1989).
25. H.N. Erten, A. Grutter, E. Rossler, H.R.von Gunten, Phys. Rev. C **25**, 2519 (1982); Nucl. Sci. Eng. **79**, 167 (1981).
26. S. Amiel, H. Feldstein, T. Izak-Biran, Phys. Rev. C **15**, 2119 (1977); T. Izak-Biran, S. Amiel, Phys. Rev. C **16**, 266 (1977); J. Inorg. Nucl. Chem. **40**, 757; 937 (1978).
27. A. Ramaswami, V. Natarajan, B.K. Srivastava. R.H. Iyer, J. Inorg. Nucl. Chem. **43**, 3067 (1981); R.H. Iyer, C.K. Mathews, N. Ravindran, K. Rengan, D.V. Singh, M.V. Ramaniah, H.D. Sharma, J. Inorg. Nucl. Chem. **25**, 465 (1963).
28. K. Persyn, E. Jacobs, S. Pomme, D. De Frenne, K. Govaert, M.L. Yoneama, Nucl. Phys. A **620**, 171 (1997).
29. S. Pomme, E. Jacobs, K. Persyn, D. De Frenne, K. Govaert, M.L. Yoneama, Nucl. Phys. A **560**, 689 (1993); S. Pomme, E. Jacobs, M. Piessens, D. De Frenne, K. Persyn, K. Govaert, M.L. Yoneama, Nucl. Phys. A **572**, 237 (1994).
30. R.H. Iyer, H. Naik, A.K. Pandey, P.C. Kalsi, R.J. Singh, A. Ramaswami, A.G.C. Nair, Nucl. Sci. Eng. **135**, 227 (2000); H. Naik, A.G.C. Nair, P.C. Kalsi, A.K. Pandey, R.J. Singh, A. Ramaswami, R.H. Iyer, Radiochim. Acta **75**, 69 (1996).
31. K. Wolfsberg, J. Inorg. Nucl. Chem. **37**, 1125 (1975).
32. S.J. Balestrini, L. Forman, Phys. Rev. C **10**, 1872 (1974).
33. E. Dobreva, N. Menoff, J. Radioanal. Nucl. Chem. Art. **81**, 29 (1984).
34. C. Hameli, PhD Thesis, Grenoble 1983.
35. M. Haddad, J. Crancon, G. Lhospice, M. Asghar, Radiochim. Acta **46**, 23 (1989).
36. A. Notea, Phys. Rev. **182**, 1331 (1969).

37. S.M. Qaim, H.O. Denschlag, J. Inorg. Nucl. Chem. **32**, 1767 (1970); H.O. Denschlag, S.M. Qaim, Z. Naturforsch. A **24**, 2000 (1969).
38. S. Amiel, H. Feldstein, Phys. Rev. C **11**, 845 (1975); in *Proceedings of the third IAEA Symposium on Physics and Chemics of Fission, Rochester*, Vol. **II** (IAEA, Vienna, 1973) p. 65.
39. A.C. Wahl, At. Data Nucl. Data Table **39**, 1 (1988); A.C. Wahl, Phys. Rev. C **32**, 184 (1985); A.C. Wahl, J. Radioanal. Chem. **55**, 111 (1980); A.C. Wahl, A.E. Norris, R.A. Rouse, J.C. Williams, in the *Proceedings of the second IAEA Symposium on Physics and Chemics of Fission, Vienna* (IAEA, Vienna, 1969) p. 813.
40. J. Blachot, J. Crancon, J. Hamelin, Ch. Hamelin, A. Moussa, in *Proceedings of the fourth IAEA Symposium on Physics and Chemics of Fission, Julich*, SM-241/F29 (IAEA, Vienna, 1979).
41. M. Haddad, J. Crancon, G. Lhospice, M. Asghar, Nucl. Phys. A **481**, 333 (1988).
42. J.K. Dickens, J.W. McConnell, Phys. Rev. C **23**, 331 (1981).
43. R.M. Harbour, D.E. Troutner, K.W. MacMurdo, Phys. Rev. C **10**, 769 (1974); D.E. Troutner, R.M. Harbour, Phys. Rev. C **4**, 505 (1971); J. Inorg. Nucl. Chem. **34**, 801 (1972).
44. J.K. Dickens, J.W. McConnell, Phys. Rev. C **24**, 192 (1981).
45. H. Gaggeler, H.R. von Gunten, Phys. Rev. C **17**, 172 (1978);
46. H.H. Meixler, K. Wolfsberg, H.O. Denschlag, Can. J. Chem. **61**, 665 (1983).
47. S.B. Manohar, A. Ramaswami, B.K. Srivastava, A.V.R. Reddy, A.G.C. Nair, G.K. Gubbi, A. Srivastava, SatyaPrakash, Nucl. Phys. A **502**, 307 (1989).
48. H.N. Erten, N.K. Aras, J. Inog. Nucl. Chem. **41**, 149 (1979).
49. R. Vandenbosch, J.R. Huizenga, *Nuclear Fission* (Academic Press, Inc, New York and London, 1973) p. 322.
50. F. Gonnenwein, *Mass, charge and kinetic energy of fission fragments*, in C. Wagemans, *The Nuclear Fission Process* (CRC Press, London, 1991) p. 392.
51. K.F. Flynn, Argone National Laboratory Report, ANL-75-24 (1975).
52. E. Browne, R.B. Firestone, *Table of Radioactive Isotopes*, edited by V.S. Shirley (Wiley, New York, 1986).
53. J. Blachot, Ch.Fiche, *Table of Radioactive Isotopes and their main decay characteristics*, Ann. Phys. **6**, 3 (1981).
54. B.F. Rider, *Compilation of Fission Products Yields*, Vallecitos Nuclear Centre Report, NEDO 12154 3c ENDF-327 (1981); T.R. England, B.F. Rider, *Evaluation and Compilation of Fission Products Yields*, ENDF/BVI (1989).
55. M. James, R. Mills, *Neutron Induced Fission Yiolds*, UKFY2 (1991).
56. E.K. Hyde, *The Nuclear Properties of the Heavy Elements*, Vol. **III** (Presentic Hall, Englewood Cliffs, New Jersey, 1964) p. 215.
57. B.D. Wilkins, E.P. Steinberg, R.R. Chasman, Phys. Rev. C **14**, 1832 (1976).
58. J.R. Nix, Nucl. Phys. A **130**, 241 (1969).
59. H. Nifenecker, J. Phys. Lett. **41**, 47 (1980); H.A. Nifenecker, J. Blachot, J.P. Bocquet, R. Brissot, J. Crancon, C. Hamelin, G. Mariolopoulos, C. Ristori, in *Proceedings of the fourth IAEA Symposium on Physics and Chemics of Fission, Julich*, Vol. **II** (IAEA, Vienna, 1979) p. 35.
60. M. Asghar, Z. Phys. A **296**, 79 (1980); M. Asghar, R. W. Hasse, J. Phys. C **6**, 455 (1984).
61. M. Berlanger, A. Gobbi, F. Hanappe, U. Lynen, C. Ngo, A. Olmi, H. Sann, H. Stelzer, H. Richel, M.F. Rivet, Z. Phys. A **291**, 133 (1979).
62. U. Brosa, H.J. Krappe, Z. Phys. A **284**, 65 (1978).
63. E. Rejmund, A.V. Ignatyuk, A.R. Junghans, K.H. Schmidt, Nucl. Phys. A **678**, 215 (2000).
64. P. Schillebeeckx, C. Wagemans, A.J. Deruytter, R. Barthelemy, Nucl. Phys. A **545**, 623 (1992).
65. J. Blons, C. Mazur, D. Paya, M. Ribrag, H. Weigmann, Nucl. Phys. A **414**, 1 (1984).
66. H. Nifenecker, G. Mariolopoulos, J.P. Bocquet, R. Brissot, Ch. Hamelin, J. Crancon, Ch. Ristori, Z. Phys. A **308**, 39 (1982).
67. D.L. Hill, J.A. Wheeler, Phys. Rev. **89**, 1102 (1969).